AD NUMBER

AD091695

NEW LIMITATION CHANGE

TO

Approved for public release, distribution unlimited

FROM

Distribution authorized to U.S. Gov't. agencies and their contractors; Administrative/Operational Use; 1956. Other requests shall be referred to Office of Naval Research, Arlington, VA 22203.

AUTHORITY

ONR ltr dtd 26 Oct 1977

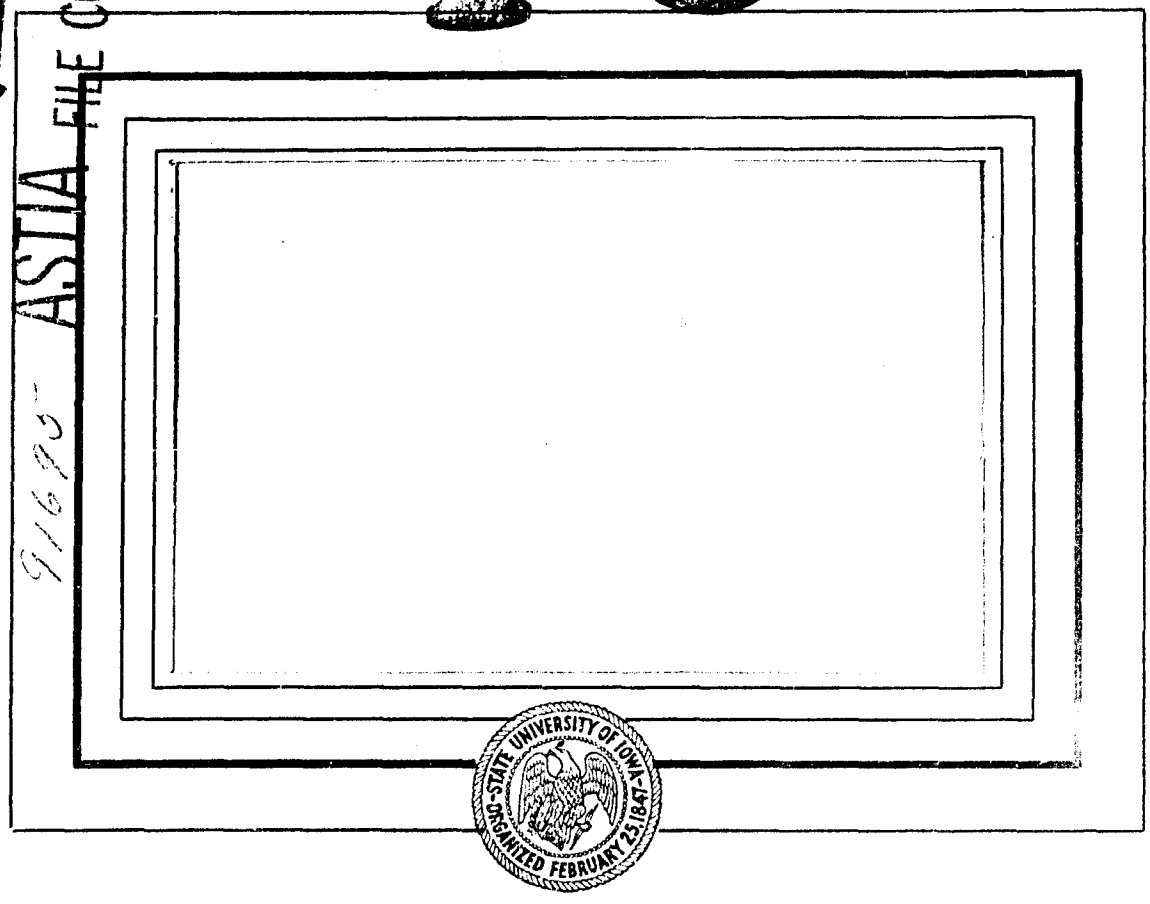

Department of Physics

STATE UNIVERSITY OF IOWA

Iowa City

"A New Determination of the Intensities of Primary Cosmic Ray Alpha Particles and Li, Be, B Nuclei at $\lambda = 41.5°$ Using a Cerenkov Detector"*

by

William R. Webber

Department of Physics
State University of Iowa
Iowa City, Iowa

*Assisted by a joint program of the Office of Naval Research and the Atomic Energy Commission.

Abstract

Measurements of the intensities of the alpha particles and Li, Be, B nuclei in the primary cosmic radiation have been made at an average atmospheric depth of 18.5 g/cm^2 in two "Skyhook" balloon flights at $\lambda = 41.5°$. The measuring instrument consisted of a thin (3.0 g/cm^2) Cerenkov detector placed within the solid angle of a Geiger counter telescope. This detector yielded unusually good resolution of the alpha particle and Li, Be, B components. This fact and the slow rate of rise of the two balloons made possible a detailed determination of the dependence of alpha particle intensity on atmospheric depth. The quality of the data justified a new approach to the problem of extrapolating the alpha particle intensity to the top of the atmosphere. This extrapolation was carried out by applying a "diffusion" equation of the type previously used for nuclei with $Z > 2$ to the observed pressure-altitude dependence of alpha particle intensity. The resulting estimate of the alpha particle intensity at the top of the atmosphere is significantly lower than previous estimates.

At 18.5 g/cm^2 the sum of the vertical intensities of the Li, Be, B components was found to be 3.11 ± 0.31 (m^2 steradian sec)$^{-1}$ and the intensities $J_{Li}/J_{Be}/J_B$ were found to be as 3/4/2. The (light nuclei/medium nuclei) intensity ratio at the top of the atmosphere as determined by this experiment was 0.35 ± 0.09.

The vertical intensities at the top of the atmosphere

of the various components of the primary radiation as obtained in this experiment at $\lambda = 41.5°$ were:

Component	J^o $(m^2\text{-steradian-sec})^{-1}$
Protons	≤ 526
Alpha Particles	74 ± 5
Li, Be, B	2.28 ± 0.55
$Z \geq 6$	9.2 ± 1.2

I. Introduction

Due to its unique properties, the Cerenkov detector is being used increasingly in experiments requiring charge determination of the cosmic radiation in the upper atmosphere.[1] Most important of these properties is the fact that

---

[1] See W. R. Webber and F. B. McDonald, Phys. Rev. 100, 1460 (1955) for a discussion of the Iowa work leading up to the present experiment and for a summary of the work of other experimenters using Cerenkov detectors to measure the primary radiation in the upper atmosphere.

---

the output from a Cerenkov detector, in the form of visible electromagnetic radiation, is proportional to $Z^2\left(1-\frac{1}{\beta^2 n^2}\right)$, where Z is the charge of the incident particle, βc is its velocity and n is the index of refraction of the medium. Thus in a Cerenkov detector one has the advantage of a Z^2 charge dependence similar to ionization detectors; but the Cerenkov output decreases with decreasing β, in distinct contrast to the Z^2/β^2 output of ionization detectors. As a result, low energy singly charged particles, which are indeed plentiful in the upper atmosphere, do not contribute to the background in the range of outputs characterizing high energy alpha particles and Li, Be, B nuclei in a Cerenkov detector. Hence, one can obtain much more certain identification of these components than by any method depending upon ionization alone.

A second important property of a Cerenkov detector is

the fact that the optical radiation is emitted in the forward direction in a cone of half angle α given by $\cos \alpha = \frac{1}{\beta n}$. This means that the Cerenkov detector can function as a directional device and thus can be used to provide discrimination against upward moving albedo particles.

A main disadvantage of Cerenkov detectors as used for cosmic ray research in the upper atmosphere has been their somewhat poor charge resolution in the low Z region. This is due partly to the necessity for using thin radiating materials (to minimize nuclear interactions) and partly to the inherently low light output from the Cerenkov effect-both effects tending to introduce wide statistical fluctuations in the photomultiplier tube output for particles of the same β.

By careful choice of the photomultiplier tube and by control of the various parameters affecting this statistical fluctuation it has been possible to create a unit with unusually good charge resolution. Using a one inch thick Lucite radiator, pulse height distributions with half widths (width at half height divided by the magnitude of the pulse height at the maximum of the distribution) of 35% were consistently obtained using sea level μ-mesons as a beam of high energy particles. Since the half widths of the individual charge distributions may be expected to be roughly proportional to $1/Z$ (due to Z^2 increase in light output and consequent improvement in photomultiplier statistics) this indicated that very satisfactory resolution could be expected for the individual charge components in the alpha particle and Li, Be, B pulse height regions.

THIS
PAGE
IS
MISSING
IN
ORIGINAL
DOCUMENT

traces on the CRT, provided by the deflections of the spot (the spot was intensified only when a telescope coincidence was recorded), provided a quantitative measure of the amount of Cerenkov light emitted by the particles as they passed through the Lucite block. Maximum deflection, corresponding to saturation of the amplifier, gave a 6.3 cm trace on the CRT and corresponded to a particle with $Z \geq 6$.

The passage of a particle through the telescope accompanied by a simultaneous guard or shower pulse caused the ensuing trace on the CRT to be marked in such a manner that one could tell which group of counters ("top" or "bottom") had been triggered. Such a count was called a "J" count after the shape of the trace. Traces unaccompanied by "J" markings were called regular counts.

III. Discussion of the Effect of Nuclear Interactions and Knock-On Electrons Occurring in the Local Material of the Telescope

A. Nuclear Interactions

The average telescope particle passed through 5.5 g/cm^2 between the 2.5 g/cm^2 "identification" level in the Lucite block and the lower telescope tray. A specific fraction of these particles will have nuclear interactions in this region. A correction for these interactions must be made since we are interested in the number of regular counts at the "identification" level--not at the level of the lower telescope tray. These interacting particles should appear as "J" counts principally in the bottom "J" pulse height distribution. Since these particles have passed through the Lucite block in a normal manner they should give a pulse height distribution similar to that for regular counts. This so-called "structure" should appear superimposed on the general background of counts in the bottom "J" pulse height distribution. Indeed, this "structure" will help identify these particles, as will be seen later on.

No regular count would be expected from a particle passing through either the bottom or top tray at large angles and having nuclear interactions in the local material since at least one of the guard or shower counters should be triggered by the secondaries from such an event--thus giving a "J" count. If some of these particles happen to pass through Lucite block, some of these "J" counts should also show "structure."

Table I

Corrections Due to Nuclear Interactions

Occurring in the Counter Telescope

	Amount of Material	Z	MFP(g/cm^2)	Correction to Regular Counts (% of J18.5)	Structure Counts (% of J18.5)
Telescope Events	5.5 g/cm^2	1	80	+ 6.6	6.6
		2	50	+10.4	10.4
		3,4,5	36	+14.2	14.2
		6	24	+20.5	20.5
Non-Telescope Events (Large Angles)	3.0 g/cm^2	--	--	No	Yes (some)

interactions in the telescope.

B. Knock-on Electrons

The problem presented by knock-on electrons produced in the material of the telescope by the incident particles is two-fold. In one case the knock-ons can cause a lower guard or shower counter to be triggered simultaneously with the passage of the primary particle through the telescope--thus causing a "J" count to occur in place of a regular count. In the other case particles passing through the top tray and Lucite block at large angles such that their trajectories miss the bottom tray may produce knock-ons in the telescope. These knock-ons may in turn pass through the bottom tray thus causing regular counts. This effect, which tends to enlarge the geometric factor of the Geiger counter telescope, has recently been discussed by Linsley in connection with the measurement of the intensities of heavy primaries by Geiger counter telescopes.[2]

---

[2] J. Linsley, Phys. Rev. 97, 1292 (1955).

The bottom guard counters will tend to minimize this effect somewhat by recording as "J" counts many of these particles. It should be noted that the above two knock-on effects tend to cancel one another. All the "J" counts caused by these knock-ons should show "structure" since presumably the primary particles have passed through the Lucite block in normal manner, even though in some cases they may have missed the lower telescope tray.

An effect analogous to the above effects may occur in the top tray and surrounding guard counters due to back

scattered electrons produced in the telescope. The evidence, both theoretical and experimental, indicates this effect is small, however.

A theoretical analysis of the effect of knock-on electrons has been carried out using a modified Rutherford formula[3] to

---

[3]B. Rossi, High Energy Particles (Prentice-Hall, Inc., New York, 1952), p. 14-23.

---

find the probability per unit path length in the telescope that a knock-on of a given energy is produced. If one folds in the energy spectrum of the primary radiation and the range-energy relation for the knock-on electrons,[4] the probability

---

[4]L. R. Glendenin, Nucleonics, 2, No. 1, 12 (1948).

---

that a knock-on electron with energy great enough to penetrate the bottom counters will emerge from the local material can be calculated as a function of the Z of the incident particle. This relation is found to be $P(Z) = 1 - e^{-0.0137Z^2}$. The work of Brown et. al.[5] on the angular distribution of knock-on

---

[5]Brown, McKay, and Palmatier, Phys. Rev. 76, 507 (1949).

---

electrons from penetrating particles (mesons) indicates a distribution of $\cos^{2.5}\theta$ for the emerging knock-on electrons where θ is the angle between the knock-on and its primary. Integrating over all possible trajectories of the primary particles

passing through the top tray and Lucite block one can then obtain the total probability that upon the passage of a particle of a given Z through the Lucite block a regular or a "J" count will be obtained.

A summary of the effects of knock-on electrons is given in Table II.

An experimental check on the above calculations for knock-on electrons can be obtained in the case of sea level μ-mesons. Table II predicts that 1.5% of these singly charged particles should be accompanied by "structure" type "J" counts due to knock-on electrons (no nuclear interactions present). Experimentally it is found that 1.7% ± 0.3% of the μ-mesons are indeed accompanied by "structure" type bottom "J" counts.

In later sections, as a check on the preceeding calculations, the experimentally observed "J" "structure" for each charge component will be compared with that expected due to knock-on electrons and nuclear interactions.

Table II

Corrections Due to Knock-On Electrons

Occurring in the Counter Telescope

Z		1	2	3,4,5	6
Correction to Regular Counts (% of J18.5)	Telescope Events	+1.1	+2.6	10.0	48.2
	Non-Telescope Events (Large Angles)	-0.4	-0.9	- 3.7	-20.8
Total		+0.7	+1.7	+ 6.5	+34.5
Structure Counts (% of J18.5)	Telescope Events	+1.1	+2.6	10.0	48.2
	Non-Telescope Events	+0.4	+0.9	3.7	20.8
Total		1.5	3.5	13.3	59.0

IV. Balloon Flights

The apparatus, enclosed in an airtight aluminum cylinder, was flown by balloon from San Angelo, Texas ($\lambda = 41.5°$) on January 12th and 19th, 1955. A feature of both flights was the very slow rise of the balloons to altitude, thus enabling good statistics to be obtained on the variation of the various cosmic ray charge components with atmospheric depth. Both flights reached maximum altitude at approximately 10 A.M. local time and remained nearly level at this altitude for 5 hours before the apparatus was released and parachuted to earth. Flight I maintained an average altitude of 90,200 ft. (17.5 g/cm^2) during this 5 hour period while Flight II averaged 94,300 ft. (14.5 g/cm^2). The atmospheric pressure as a function of time was determined by photographing a Wallace and Tiernan pressure gauge and a watch at 2 minute intervals. The pressure determined in this manner agreed to within $\pm$ 1.0 g/cm^2 at maximum altitude on both flights with independent measurements supplied by Winzen Research, Inc.

V. Experimental Results

Data from the two flights were first analyzed separately, but since the separate results were consistent in every way, the data have been combined in this paper.

A breakdown of the results obtained at maximum altitude for Flights I and II (18.5 g/cm^2 average depth-including 16.0 g/cm^2 of air + 2.5 g/cm^2 correction due to local material and finite opening angle of telescope) according to apparent Z and type of count is shown in Table III.

A. Alpha Particles

The pulse height distributions in the range $2h_o \leq h \leq 6h_o$ are shown in Fig. 3. The peak due to alpha particles at $\sim 4h_o$ is clearly evident in the distribution of regular counts. Note that even if all "J" and regular counts in this region are grouped into a single pulse height distribution a partially resolved alpha peak is still obtained, the only discrimination involved being the inherent discrimination of a Cerenkov counter against slow particles. An improvement in resolution by a factor of 2 is obtained, however, when only regular counts are considered. This indicates that the guard and shower counters are successfully identifying many non-alpha events in this pulse height region.

As a first step in the determination of the number of counts that can actually be attributed to alpha particles we arbitrarily consider the pulse height region $2.6h_o \leq h \leq 5.6h_o$ as the alpha particle region. Within this region, combining the results of Flights I and II, a total of 1527 regular counts were obtained. To this value we must make the following

Table III

Raw Data Obtained at Maximum Altitude (Flights I and II) Grouped According to Apparent Z

Pulse Height	Counts					
	Flight I			Flight II		
	Regular	Top "J"	Bott "J"	Regular	Top "J"	Bott "J"
0	2,940	572	504	2,576	612	352
$0.2h_o^* \leq h \leq 2.6h_o$ ($Z = 1$)	15,243	1,017	1,777	14,259	1,196	1,901
$2.6h_o \leq h \leq 6.0h_o$ ($Z = 2$)	739	169	304	788	224	370
$7.0h_o \leq h \leq 15h_o$ ($Z = 3,4,5$)	44	45	60	52	48	62
$h \geq 15h_o$ ($Z \geq 6$)	46	86	97	47	93	110
Totals	19,012	1,889	2,722	17,732	2,173	2,795

Note: Time intervals are identical for Flights I & II.

corrections:

(1) Interpolation between singly and doubly charged distributions. This interpolation is facilitated by the fact that, on theoretical grounds, the singly charged "tail" at high altitude should be very similar to the "tail" observed on the μ-meson distribution at sea level. One has only to normalize the two distributions and subtract out the μ-meson tail. Data obtained as the balloons rose to altitude corroborate this method of correction: viz., in the region below 150 g/cm^2, where protons would be expected to be quite abundant and the composition of the singly charged group would be more nearly like that at maximum altitude, the normal sea level μ-meson "tail" was observed. Above this depth, as the alpha particles became more plentiful the pulse height region above $2h_o$ steadily filled out and the structure of the alpha peak became more and more apparent with increasing altitude. (See Fig. 4).

The correction for the proton tail adds 155 ± 50 counts lying between $h = 2h_o$ and $h = 2.6h_o$ to the regular alpha particle distribution.

(2) Correction due to knock-on electrons and nuclear interactions occurring in the telescope. The correction due to these effects has been discussed in a previous section and amounts to +12.1% of the total number of alpha particle counts or an addition of 230 ± 40 counts to the regular alpha particle distribution.

We are now in a position to compare our theoretical estimates on the effect of nuclear interactions and knock-on

electrons occurring in the telescope with the experimental results. In the previous section it was estimated that at least 12.8% of the total number of alpha particle counts should appear as "structure" in the lower "J" pulse height distribution. Reference to Fig. 3 shows that this "structure" is indeed present and contains approximately 260 counts or 13.7% of the total number of alpha particle counts--a result in close agreement with the predicted value. Note that the "J" distribution from the top guard and shower counters shows no "structure." This would be expected since the products of the events showing a pulse height structure generally would not be expected to reach these counters.

(3) Background in the regular alpha particle distribution due to inefficiency of guard and shower devices. Any such inefficiency would allow events that are not due to true alpha particles to appear as background in this region of the regular distribution.

Since at sea level (no interactions) and in the atmosphere below 150 g/cm^2 (where proton interactions occur but alpha particles are absent) all counts in the region $2.0h_o \leq h \leq 6.0h_o$ should be "J" counts, (save the well defined singly charged tail) a measure of the efficiency of the detection system for "J" type events can be gained by comparing the number of regular and "J" counts obtained in this pulse height region at these altitudes. The results--2 regular counts and 31 "J" counts--indicate that the guard and shower system is $93 \pm 4\%$ efficient in detecting background events lying in the alpha particle pulse height region. This value for the efficiency is

corroborated by the number of background events lying in the regular distribution from $7h_0 \leq h \leq 15h_0$. In this pulse height region it is found that the guard and shower system is $\sim 97\%$ efficient in detecting "J" type events. This slightly higher efficiency can be accounted for by the fact that the guard and shower system tends to become more efficient the larger the background event being considered.

At altitude approximately 1000 "J" events occurred in the alpha particle pulse height region. Thus 70 ± 40 undetected "J" events must lie in the alpha particle region as background. These counts must be subtracted from the regular alpha particle distribution.

(4) Alpha particle tail above $5.6h_0$. This accounts for an estimated additional 45 ± 10 counts.

Thus we have a grand total of $1527 + 360 = 1887 \pm 110$ (statistical and experimental errors included) alpha particle counts at a depth of 18.5 g/cm^2. To extrapolate this value to the top of the atmosphere we must take cognizance of the fact that an appreciable fraction of these alphas may be fast fragments from collisions of the heavier components in the atmosphere above the apparatus. A straight exponential extrapolation is not appropriate and one should consider the diffusion equations for the alpha particles. Neglecting ionization loss and assuming energy independence for the parameters λ_I, $P_{I,I}$ these are, (after notation of Noon and Kaplon).[6]

---

[6] J. H. Noon and M. F. Kaplon, Phys. Rev. 97, 769 (1955).

$$\frac{dJ_I(x)}{dx} = -\frac{J_I(x)}{\lambda_I} + \sum_{I' \geq I} \frac{P_{I'I} J_{I'}(x)}{\lambda_{I'}}$$

where I = H,M,L,α and x is the vertical depth below the top of the atmosphere. The definition and values of the parameters used in these equations may be found in the appendix.

The solution of this equation for alpha particles is:

$$J_\alpha'(x) = J_\alpha^\circ e^{-x/\lambda_\alpha'} + \left\{\frac{\lambda_L'\lambda_\alpha' P_{L\alpha}}{(\lambda_\alpha'-\lambda_L')\lambda_L}\right\}\left[J_L^\circ + \frac{\lambda_M'\lambda_L' P_{ML}}{(\lambda_L'-\lambda_M')\lambda_M} J_M^\circ + \frac{\lambda_H'\lambda_L'}{(\lambda_L'-\lambda_H')\lambda_H} J_H^\circ \right.$$

$$\left. \left(P_{HL} + \frac{\lambda_M'\lambda_L' P_{HM} P_{ML}}{(\lambda_L'-\lambda_M')\lambda_M}\right)\right]\left(e^{-x/\lambda_\alpha'} - e^{-x/\lambda_L'}\right) + \left\{\frac{\lambda_M'\lambda_\alpha'}{(\lambda_\alpha'-\lambda_M')\lambda_M}\left(P_{ML} - \frac{\lambda_M'\lambda_L' P_{ML} P_{L\alpha}}{(\lambda_L'-\lambda_M')\lambda_L}\right)\right\}$$

$$\left[J_M^\circ + \frac{\lambda_H'\lambda_M' P_{HM}}{(\lambda_M'-\lambda_H')\lambda_H} J_H^\circ\right]\left(e^{-x/\lambda_\alpha'} - e^{-x/\lambda_M'}\right) + \left\{\frac{\lambda_H'\lambda_\alpha'}{(\lambda_\alpha'-\lambda_H')\lambda_H} J_H^\circ\right\}\left[P_{H\alpha} - P_{HM}P_{M\alpha}\frac{\lambda_H'\lambda_M'}{(\lambda_M'-\lambda_H')\lambda_M}\right.$$

$$\left. - P_{HL}P_{L\alpha}\frac{\lambda_H'\lambda_L'}{(\lambda_L'-\lambda_H')\lambda_L} + P_{HM}P_{ML}P_{L\alpha}\left(\frac{\lambda_H'\lambda_M'}{(\lambda_M'-\lambda_H')}\frac{\lambda_M'\lambda_L'}{(\lambda_L'-\lambda_M')} - \frac{\lambda_H'\lambda_L'}{(\lambda_L'-\lambda_H')}\frac{\lambda_M'\lambda_L'}{(\lambda_L'-\lambda_M')}\right)\right]\left(e^{-x/\lambda_\alpha'} - e^{-x/\lambda_H'}\right)$$

In the above expression the first term on the right hand side represents the absorption of the incident alpha particle flux whereas the other terms represent contributions to this flux at a depth x due to interactions of the heavier nuclei.

Using the parameters listed in the appendix we still have two undetermined quantities, J_α° and λ_α. Due to the aforementioned slow rise of the balloons, satisfactory statistics were obtained on the intensity of alpha particles as a function of depth above 120 g/cm^2 (Figs. 4 and 5). If we choose J_α° and λ_α to give agreement with the experimental data at 18.5 g/cm^2 and with the best least squares fit to the

data as a function of atmospheric depth we find,

$$J_\alpha^o = 74 \pm 5 \ \frac{\text{alpha particles}}{m^2\text{-steradian-sec}}$$

$$\lambda_\alpha = 46.5 \pm 3.0 \ g/cm^2$$

To directly compare the results of this experiment with those obtained previously by other experimenters at this latitude it is necessary to extrapolate the known intensity at 18.5 g/cm^2 to the top of the atmosphere (M.F.P. = 45 g/cm^2) without benefit of the fragmentation correction. This extrapolation gives $J_\alpha^o = 86 \pm 5$ alpha particles $/m^2$-steradian-sec. The correction due to the fragmentation of the heavier nuclei thus reduces the alpha particle intensity at the top of the atmosphere by $14 \pm 4\%$ for experiments made at this altitude. Corresponding reductions are necessary at other altitudes and latitudes. The error on the fragmentation correction listed above comes about by considering the errors on the individual parameters in the diffusion equation for alpha particles. (See section V-B and the appendix). This propagation of errors analysis indicates that such a fragmentation correction is justified by the accuracy of the present data,

Note that, as a consequence of the production of secondary alphas, the absorption of alpha particles deviates considerably from an exponential in the uppermost region of the atmosphere, although below 18.5 g/cm^2 the absorption is approximately exponential with an apparent M.F.P. of 58 g/cm^2. A balloon flight at 120,000 feet (7.5 g/cm^2 including material) should be decisive in confirming this non-exponential absorption

in the extreme upper region of the atmosphere.

Table IV summarizes the work to date of various observers on the alpha particle component of the primary radiation at $\lambda = 41°$. A weighted average, based on the experimental values quoted by these observers gives a value of 90.0 ± 3.0 alpha particles/m^2-steradian-sec at this latitude, (uncorrected for fragmentation).

A review of the situation with regard to the integral intensity-energy spectrum for alpha particles in the latitude sensitive region [13-20] is shown in Fig. 6.

---

[13] E. P. Ney and D. M. Thon, Phys. Rev. 81, 1068 (1951).

[14] Davis, Caulk and Johnson, Phys. Rev. 101, 801 (1956).

[15] F. B. McDonald, Private communication to E. P. Ney (1953).

[16] C. J. Waddington, Phil. Mag. 45, 1312 (1954).

[17] B. Peters, Proc. Indian Acad. of Sciences 40, 231 (1954).

[18] M. A. Pomerantz, J. Franklin, Inst. 258, 443 (1954).

[19] G. W. McClure, Phys. Rev. 96, 1391 (1954).

[20] S. F. Singer, Phys. Rev. 80, 47 (1950).

As in the case of the $\lambda = 41°$ intensity a weighted average of the experimental data is made to determine the intensity at each latitude where more than one observation has been made. The errors on these average intensitites have been assigned in accordance with the reliability of the experimental data at each latitude. Notice that the situation at $\lambda = 55°$ and $\lambda = 41°$ is much better than at the other latitudes, particularly near the equator. A spectrum of the form

Table IV

Comparison of Primary Alpha Particle Intensities Obtained at the Top of the Atmosphere by Different Observers (λ = 41°N) (Uncorrected for Fragmentation)

Author	Ref.	Method	Lat.	Alpha Particle Intensity (Particles/M^2-Steradian-Sec)	
Webber McDonald	1	Cerenkov Detector	41.5°	82 ± 9	
Webber	-	Cerenkov Detector	41.5°	86 ± 5	Weighted
Bohl	7	Double Scintillator	41.5°	90 ± 10	Average
Linsley	8	Cerenkov Det + Cl. Cham.	41.5°	88 ± 8	90.0 ± 3.0
McDonald	9	Cerenkov Det + Scint.	41.5°	96 ± 9	
Horowitz	10	Cerenkov Detector	41.5°	99 ± 15	
Perlow et. al.	11	Proportional Counters	40.0°	110 ± 20	
Bradt and Peters	12	Photographic Emulsions	41.7°	138 ± 20	

[7]L. Bohl, Ph.D. Thesis, University of Minnesota (1954).
[8]J. Linsley, Phys. Rev. 101, 826 (1956).
[9]F. B. McDonald, Private communication (1956).
[10]M. Horowitz, Phys. Rev. 98, 165 (1955).
[11]G. J. Perlow, et. al., Phys. Rev., 88, 321 (1953).
[12]H. Bradt and B. Peters, Phys. Rev. 77, 54 (1950).

$N(\epsilon) = K/(1+\epsilon)^{\alpha}$ where ϵ is the kinetic energy per nucleon is used to fit the data. The value of α is chosen to be 1.4 in accordance with the value deduced by Kaplon[21] for particles

---

[21] M. F. Kaplon et. al., Phys. Rev. 85, 295 (1952).

---

with $Z \geq 6$. The points at $\lambda = 55°$ and $\lambda = 41°$ are in good agreement with such a value for α and do not permit a variation of much more than $\pm$ 0.15 in the value chosen for this exponent.

The necessity for accurate intensity measurements on alpha particles near the equator in order to clarify the form of the intensity-energy spectrum for these particles in emphasized by Fig. 6.

If one corrects the alpha particle data to a constant altitude of 90,000ft(18 g/cm^2) using an absorption M.F.P. of 58 g/cm^2, and to a constant geomagnetic latitude of 41.5° using geomagnetic theory in conjunction with the energy spectrum given in Fig. 6, the resulting hourly counting rates indicate that the alpha particle intensity was constant to within $\pm$ 9% during both flights from 10 A.M. to 3 P.M. local time. In addition, the average hourly counting rates of alpha particles for the two flights agreed to within $\pm$ 2% during this time interval.

B. Li, Be, B Nuclei

Before we consider the observations on nuclei heavier than alpha particles, the pulse height calibration will be discussed, since the impending results depend more on pulse size information than those presented so far. Due to the non-linearities

in the system it was also necessary to know that the gain had remained constant throughout the flights. This could be verified by measuring the amplitude of the saturation pulses on the CRT. It was found that this level varied less than ± 2% for the duration of both flights, indicating a negligible change in B+ voltage and a consequent minimal change in gain characteristics of the system.

The method of system calibration was as follows: carefully calibrated pulses measured as 4 times the average sea level μ-meson pulse were passed through the system. These pulses were compared with and adjusted slightly so as to coincide with the peak of alpha particle distribution obtained at altitude. Then a gain curve over the entire range was made using these adjusted pulses as a base and giving special emphasis to pulses 9, 16, and 25 times those for the singly charged particles. Various runs were made exploring the effect of slight errors in the adjusted alpha particle pulse height. A final calibration curve was then made by comparing photographs of the traces produced by the calibrated pulses with those obtained at maximum altitude during the two balloon flights. The arrows in Fig. 7 give the pulse height expected for relativistic Li, Be, B as determined by this system calibration.

It can be seen from the differential pulse height distribution of all counts in Fig. 7 that, while there is sone indication of Li, Be, and B peaks, the resolution is quite poor. If one examines the differential pulse height distribution of the regular counts, however, the peaks due to Li, Be, and B are now clearly resolved. If we correct for the slight alpha particle tail in the Li region and consider that 6 of the

counts in the Li, Be, B region are background for undetected "J" events (detection efficiency for "J" events determined to be $\sim 97\%$ in this pulse height region) we obtain 28 Li, 36 Be and 19 B counts or a total of 83 counts that can reasonably be attributed to light (L) nuclei. The above breakdown gives a ratio of intensities $J_{Li}/J_{Be}/J_B$ of approximately 3/4/2.

The above value for the number of light nuclei observed must be corrected for knock-on electrons and nuclear interactions occurring in the local material of the telescope. The corrections due to these effects have already been discussed in a previous section and amounted to 19.7% of the total number of light particle counts or an addition of 20 ± 5 counts to the 83 regular Li, Be, and B counts.

The observed "structure" in the bottom "J" distribution amounted to 7 Li, 14 Be and 8 B counts for a total of 29 counts or 27.7% of the total number of light particle counts obtained. This result compares favorably with the predicted value of at least 25.6% for the fraction of light particles that should appear as "structure" counts in the bottom "J" distribution. As before the top "J" pulse height distribution showed no "structure" in this region.

The total number of counts that can finally be attributed to light nuclei is thus $83 + 20 = 103 \pm 11$. This gives an intensity 3.11 ± 0.33 light nuclei/m^2-steradian-sec at 18.5 g/cm^2. Extrapolating this value to the top of atmosphere using the parameters that are given in the appendix in the diffusion equation for the light component given by Noon and Kaplon[6] gives an intensity of

$$2.28 \pm 0.55 \ \frac{\text{light nuclei}}{m^2\text{-steradian-sec}}$$

Note that the intensity of light nuclei at the top of the atmosphere is less than that at 18.5 g/cm^2 due to fragmentation of the heavier components. Fig. 8-A shows the intensity of light nuclei in the upper atmosphere at $\lambda = 41°$ as predicted by the diffusion equation using the value of J_L at 18.5 g/cm^2 obtained in this experiment. This behavior seems to be supported quantitatively by the work of the Bristol group.[22]

---

[22] D. H. Perkins, Report on work of Dainton, Fowler and Kent, Proceedings of the Duke Conference on Cosmic Radiation (1953) (unpublished).

Using the values for the intensity of medium nuclei obtained in this experiment and reported in the next section (H/M ratio of 0.33 assumed at the top of the atmosphere) and the values for the intensity of light nuclei reported above gives L/M ratios of 0.80 ± 0.09 and 0.35 ± 0.09 at 18.5 g/cm^2 and at the top of the atmosphere, respectively. If, in calculating the medium intensity, an H/M ratio of 0.5 is assumed at the top of the atmosphere the L/M ratios become 0.88 + 0.10 and 0.38 + 0.10, respectively. The L/M ratio at the top of the atmosphere as deduced from this experiment is thus only slightly dependent on the value of H/M assumed at the top of the atmosphere.

If, as a comparison, we take the latest emulsion values for the intensity of medium nuclei at this latitude[23] along with

[23]Kaplon, Noon and Racette, Phys. Rev., 96, 1408 (1954).

the values for the intensity of light nuclei obtained in this experiment the corresponding L/M ratios become 0.73 ± 0.11 at 18.5 g/cm^2 and 0.29 ± 0.11 at the top of the atmosphere.

One might ask whether the above experimental results represent a positive indication of a finite intensity of light nuclei at the top of the atmosphere or whether the uncertainties in the fragmentation parameters are such that the data are inconclusive. To examine this question further a propagation of errors analysis was made on the diffusion equation for the light nuclei. The errors in the 9 independent parameters in this equation were estimated from the work of Noon and Kaplon[6] and are given in the appendix. The results of this errors analysis showed that the fraction of light nuclei at 18.5 g/cm^2 produced by the fragmentation of heavier components in the atmosphere above can be considered uncertain by ± 25%. As a consequence, the intensity of light nuclei at the top of the atmosphere becomes 2.28 ± 0.87 (m^2-steradian-sec)$^{-1}$ when both fragmentation and statistical errors are included compared with 2.28 ± 0.55 (m^2-steradian-sec)$^{-1}$ when only statistical errors are considered, and the L/M ratio at the top of the atmosphere as deduced from this experiment (H/M ratio of 0.33 assumed at top of atmosphere) becomes 0.35 ± 0.13 compared with the value of 0.35 ± 0.09 quoted above when only statistical errors are considered. As a result of the above analysis we can conclude that the results obtained in this experiment

provide the first positive non-emulsion indication that a finite intensity of Li, Be, B nuclei is present at the top of the atmosphere.

Fig. 8-B gives a summary of L/M ratios at the top of the atmosphere as deduced from measurements of various observers[24-28]

---

[24]Dainton, Fowler and Kent, Phil. Mag. 43, 729 (1952) (est.).

[25]K. Gottstein, Phil. Mag. 45, 347 (1954) (est.).

[26]P. A. Fowler, Results reported at International Congress on Cosmic Radiation, Guanajuanto, Mexico (1955) (est.).

[27]K. Gottstein, Results reported at International Congress on Cosmic Radiation, Guanajuanto, Mexico (1955) (est.).

[28]Hourd, Fleming and Lord, Private Communication (1956).

---

in the upper atmosphere. Only the most recent available results from each group working on this problem are shown. The ratios given in the figure may differ somewhat from those reported in the literature since an attempt was made to standardize the various extrapolation procedures by using the fragmentation parameters given by Noon and Kaplon[6] throughout, in the extrapolation of the data to the top of the atmosphere by the diffusion equations. The net effect of such a standardization procedure was to reduce certain of the L/M ratios deduced at the top of the atmosphere. The results that were so affected are indicated by (est.) in the references.

It is apparent from Fig. 8-B that, despite a continuing disagreement in the ratios reported by emulsion observers, all the standardized data are reasonably consistent with a L/M

ratio of between 0.3 and 0.4. Furthermore, within the statistical accuracy of the observations, this ratio does not appear to be latitude dependent although there appears to be a slight tendency for higher L/M ratios at the higher geomagnetic latitudes.

C. Nuclei with $Z \geq 6$

Despite the fact that the pulses from particles with $Z \geq 6$ generally were "off scale," valuable information could be obtained about the total intensity of these particles.

A total of 93 "off scale" regular counts were obtained. It is assumed that all these counts are caused by legitimate particles with $Z \geq 6$ since the detection efficiency for "J" events is approaching 100% in this large pulse height region.

The correction for knock-on electrons and nuclear interactions occurring in the local material of the telescope amounts to 46.5% of the total number of $Z \geq 6$ counts. This necessitates adding 77 ± 15 counts to the 93 regular counts to take into account the above effects, giving a total of $93 + 77 = 170 \pm 20$ counts at 18.5 g/cm^2 due to nuclei having $Z \geq 6$. The corresponding intensity is 5.12 ± 0.60 $Z \geq 6$ nuclei/m^2-steradian-sec. Using the parameters in the appendix in the diffusion equations for the medium and heavy components as given by Noon and Kaplon[6] (H/M = 0.33 assumed at the top of the atmosphere) gives an intensity of

$$9.2 \pm 1.2 \ \frac{Z \geq 6 \text{ nuclei}}{\text{m}^2\text{-steradian-sec}}$$

at the top of the atmosphere. Assuming H/M = 0.5 at the top of the atmosphere gives an intensity of 9.1 ± 1.2 $Z \geq 6$ nuclei/m^2-steradian-sec. Thus the intensity of $Z \geq 6$ nuclei at the top of the atmosphere is not sensitive to the value of H/M assumed at the top of the atmosphere. The above intensity is to be regarded as less certain than those reported for the other charge components, due to the various assumptions necessitated by the fact that these pulses were "off scale." It may be compared with the intensity of 9.7 ± 1.5 $Z \geq 6$ nuclei/m^2-steradian-sec obtained at $\lambda = 41°$ using the latest emulsion techniques.[23]

D. Singly Charged Particles

To find the maximum number of counts attributable to primary protons at 18.5 g/cm^2 let us compare the singly charged pulse height distribution at this altitude with the sea-level μ-meson distribution. If the singly charged pulse height distribution at altitude was due entirely to primary protons it should have an almost identical shape to that obtained from μ-mesons at sea level. This is so because all of the factors that are believed to contribute to the half-widths of the respective pulse height distributions are equal except for that due to the variation in β of the incoming particles. This is a 15% contribution to the half width in the case of the sea level - μ meson pulse height distribution but only a 2% contribution to the half width of the pulse height distribution for primary protons near the top of the atmosphere at $\lambda = 41°$ The net effect is that the primary proton distribution should have a half width only 2% less than that for μ-mesons at sea level; or

for the present purposes the two pulse height distributions may be considered identical in shape.

Fig. 9 shows the two pulse height distributions normalized in the region $1.2h_o \leq h \leq 2.0h_o$ and superimposed. This region is chosen for normalization because few of the low energy particles at high altitude would be expected to statistically scatter into this region. All or most of the counts in this region then, should be due to the statistical scatter of the more energetic particles (presumably mostly primary protons) similar to the scatter of pulses from μ-mesons at sea level. Therefore normalization in this region should most nearly give an indication of the number of counts that can be attributed to primary protons at this altitude. It is evident from the figure that, using this normalization procedure, there is a considerable excess of counts in the low and medium pulse height regions of the singly charged distribution at 18.5 g/cm^2. It seems reasonable to attribute these counts to: (1) secondary protons with $0.5 \leq \beta \leq 0.9$, (2) mesons with $0.7 \leq \beta \leq 0.9$ and (3) upward moving albedo particles (downward to upward ratio of detector sensitivity is 2.5).

Fig. 9 indicates that only about 1/2 (13,900 counts) of the singly charged counts at 18.5 g/cm^2 lie under the normalized μ-meson curve and can therefore be reasonably attributed to downward moving primary protons or very energetic mesons and electrons, all of which will give pulses identical to those from μ-mesons at sea level. The percentage of energetic mesons and electrons at this depth in the atmosphere is not well known; therefore this method should serve only to set some sort of an

upper limit on the primary proton intensity at this altitude. To arrive at a flux value for primary protons one must take into account, as in the case of the other charge components, those primary protons having nuclear interactions in the local material of the telescope or producing knock-on electrons capable of giving "J" counts. The correction for these effects amounts to 7.3% of the total number of proton counts or an addition of 1,100 counts to the regular proton distribution.

The observed "structure" in the singly charged pulse height region of the bottom "J" distribution amounts to 1,500 counts compared with a predicted "structure" of 1,200 counts due to primary protons alone. This excess of observed "structure" counts is presumably due to those "J" counts produced by secondary particles passing through the telescope.

A maximum of 13,900 + 1,100 = 15,000 counts can reasonably be attributed to primary protons at this altitude. The corresponding intensity is ≤ 452 primary protons/m^2-steradian-sec at 18.5 g/cm^2.

To extrapolate this value to the top of the atmosphere one should take into account the production of very energetic protons by the interactions of the heavier components in the atmosphere above. This effect may be appreciable, as in the case of the alpha particle calculations, and could similarly be handled by a proton diffusion equation. Many of the important parameters involved in this equation are still relatively unknown however, and, in addition, the present data hardly warrants such a careful extrapolation.

Instead, to allow for this effect to some extent, we shall

take a generous attenuation M.F.P. for protons in air of 120 g/cm^2. This approximate extrapolation gives an estimated intensity of

$$\leq 526 \ \frac{\text{primary protons}}{m^2\text{-steradian-sec}}$$

at the top of the atmosphere.

This result, while admittedly somewhat crude, is in quantitative agreement with the recent results of Vernov and Charakhchyan[29] and Winckler and Anderson[30] which indicate a lower primary proton intensity than was originally supposed.

A tabular summary of the results of the present work is given in Table V.

---

[29] S. N. Vernov and A. N. Charakhchyan, Doklady SSSR, 91, 487 (1953).

[30] Work of J. R. Winckler and K. Anderson reported by E. P. Ney at International Congress on Cosmic Radiation, Guanajuanto, Mexico (1955).

Table V

Summary of Experimental Results ($\lambda = 41.5°$)

Component	Vertical Intensity $\frac{\text{Particles}}{m^2\text{-steradian-sec}}$		Pct. of Total Primary Radiation
	Observed at 18.5 g/cm^2	Estimated at Top of Atmosphere (Primaries)	
Protons	$\leq$ 452	$\leq$ 526	$\leq$ 86.1
Alpha Particles	57.0 $\pm$ 3.5	74 $\pm$ 5	12.1
Li, Be, B	3.11 $\pm$ 0.33	2.28 $\pm$ 0.55	0.4
$Z \geq 6$	5.12 $\pm$ 0.60	9.2 $\pm$ 1.2	1.4
Total	$\leq$ 517	$\leq$ 611	100

Appendix: Parameters Used in Diffusion Equation Extrapolations[31]

Intensities $\frac{\text{Particles}}{m^2\text{-steradian-sec}}$		M.F.P.	
$J_H^o = 2.6 \pm 0.9$[23]		$\lambda_H = 18.0$ g/cm^2	$\lambda_H' = 24.0 \pm 2.7$ g/cm^2
$J_M^o = 7.1 \pm 1.3$[23]		$\lambda_M = 26.5$ g/cm^2	$\lambda_M' = 30.5 \pm 3.6$ g/cm^2
$J_L^o = 2.28 \pm 0.25$	as determined by this experiment	$\lambda_L = 31.5$ g/cm^2	$\lambda_L' = 34.0 \pm 4.2$ g/cm^2
$J_a^o = 74 \pm 5$		$\lambda_a = 45.5$ g/cm^2	$\lambda_a' = 46.5 \pm 5.0$ g/cm^2

where $\lambda_x' = \frac{\lambda_x}{1-P_{xx}}$

Fragmentation Probabilities

$P_{HH} = 0.25 \pm 0.05$	$P_{MM} = 0.13 \pm 0.05$	$P_{LL} = 0.07 \pm 0.07$[24]	
$P_{HM} = 0.27 \pm 0.05$	$P_{ML} = 0.42 \pm 0.09$	$P_{La} = 0.5 \pm 0.3$[32]	
$P_{HL} = 0.48 \pm 0.07$	$P_{Ma} = 1.42 \pm 0.15$	$P_{aa} = 0.02$ (est.)	
$P_{Ha} = 2.07 \pm 0.15$			

---

[31] All values and errors from Noon and Kaplon, loc. cit., unless otherwise noted. The M.F.P. are considered to be accurate within ± 10%.

[32] M. F. Kaplon, private communication (1955) est.

VI. Acknowledgments

I wish to express my deepest appreciation to Professor J. A. Van Allen for his continued encouragement and interest in this work; to Dr. F. B. McDonald for his helpful advice throughout the course of this project; to R. F. Missert for his many stimulating discussions; to the members of the shop for their continued cooperation; to Winzen Research, Inc. for two very fine balloon flights; and to the Office of Naval Research and the Atomic Energy Commission for their assistance of the Iowa Cosmic Ray program.

Figure Captions

Fig. 1. Outline drawing of Geiger counter telescope and Cerenkov detector showing arrangement of guard counters.

Fig. 2. Block diagram of the electronic circuitry.

Fig. 3. Pulse height distributions of regular and "J" counts in alpha particle region at 18.5 g/cm^2 (Flights I and II combined).

Fig. 4. Differential Pulse Height Distribution of regular counts as a function of altitude in the region $1.8h_o \leq h \leq 4.4h_o$ showing the development of the alpha particle peak and extrapolation of the singly charged tail.

Fig. 5. Alpha particle intensity vs. atmospheric depth; showing extrapolation to the top of the atmosphere using the alpha particle diffusion equation.

Fig. 6. Integral intensity-energy spectrum for alpha particles in the latitude sensitive region The dashed line refers to spectrum $N(\epsilon) = 390/(1+\epsilon)^{1.4}$. The dotted line indicates the corrected spectrum obtained when fragmentation of the heavier components is considered. The numbers in the figure next to the experimental points give the reference numbers in the text of the experimental data used in calculating the weighted averages of the intensity for each latitude.

Fig. 7. Differential pulse height distribution of all counts and of regular counts in Li, Be, B region at 18.5 g/cm^2.

Fig. 8A. Intensity of light nuclei in the upper atmosphere

at $\lambda = 41°$ as predicted by the diffusion equation for light nuclei using the value of $N_L(18.5)$ obtained in this experiment.

Fig. 8B. Summary of L/M ratios deduced at the top of the atmosphere from the work of various experimenters. All extrapolations to the top of the atmosphere are standardized using the fragmentation parameters given by Noon and Kaplon[6] and therefore may differ slightly from those reported in the literature. The numbers in figure next to the experimental points refer to the reference numbers in the text.

Fig. 9. Determination of an upper limit on primary proton intensity at 18.5 g/cm^2 by superimposing the sea level μ-meson distribution on the singly charged distribution obtained at 18.5 g/cm^2 (Flights I and II combined. Distributions normalized in $1.2h_o \leq h \leq 2.0h_o$ pulse height region).

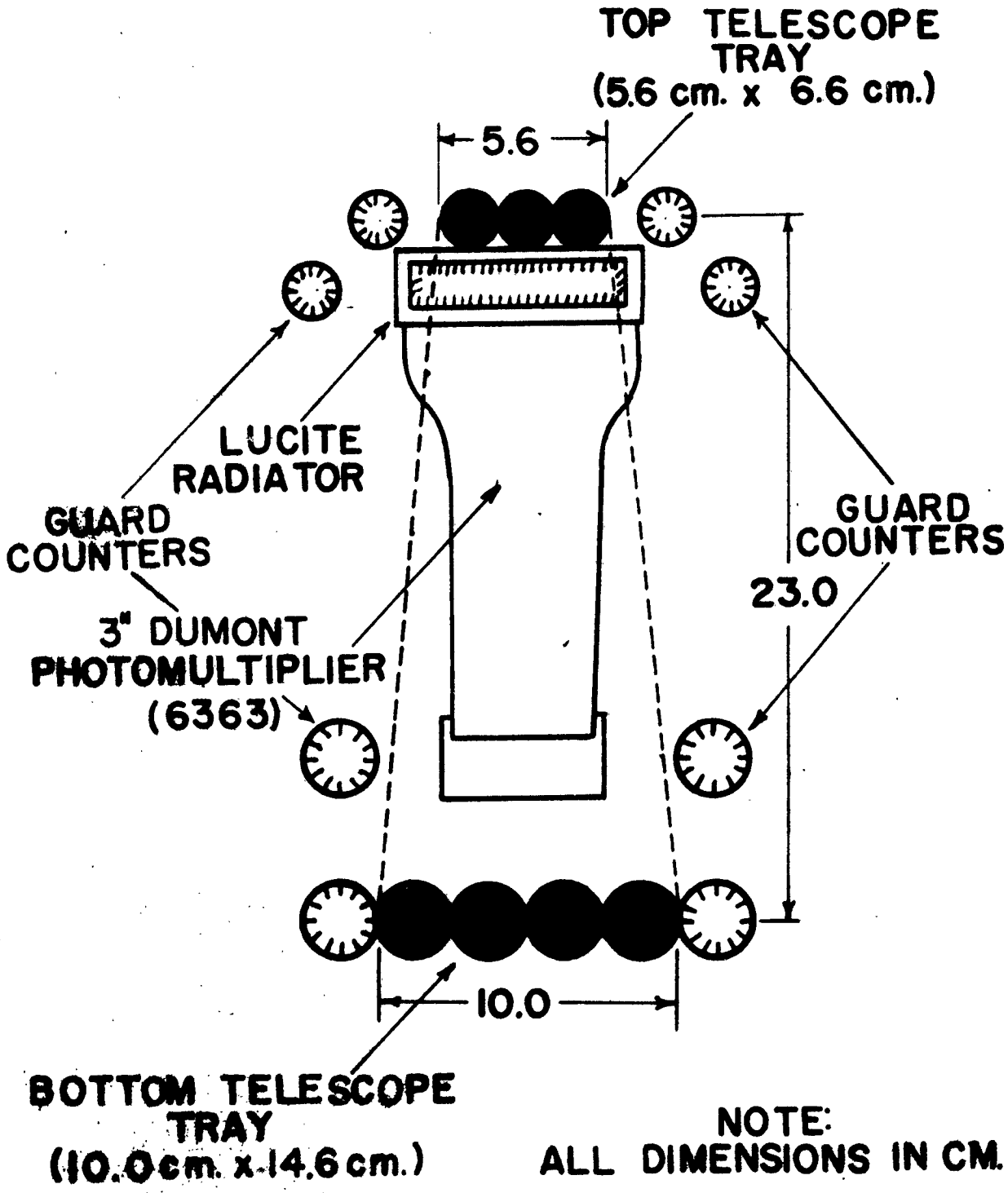
TOP TELESCOPE TRAY
(5.6 cm. x 6.6 cm.)
5.6
LUCITE RADIATOR
GUARD COUNTERS
3" DUMONT PHOTOMULTIPLIER (6363)
GUARD COUNTERS
23.0
10.0
BOTTOM TELESCOPE TRAY
(10.0cm. x 14.6 cm.)
NOTE:
ALL DIMENSIONS IN CM.

FIGURE 1

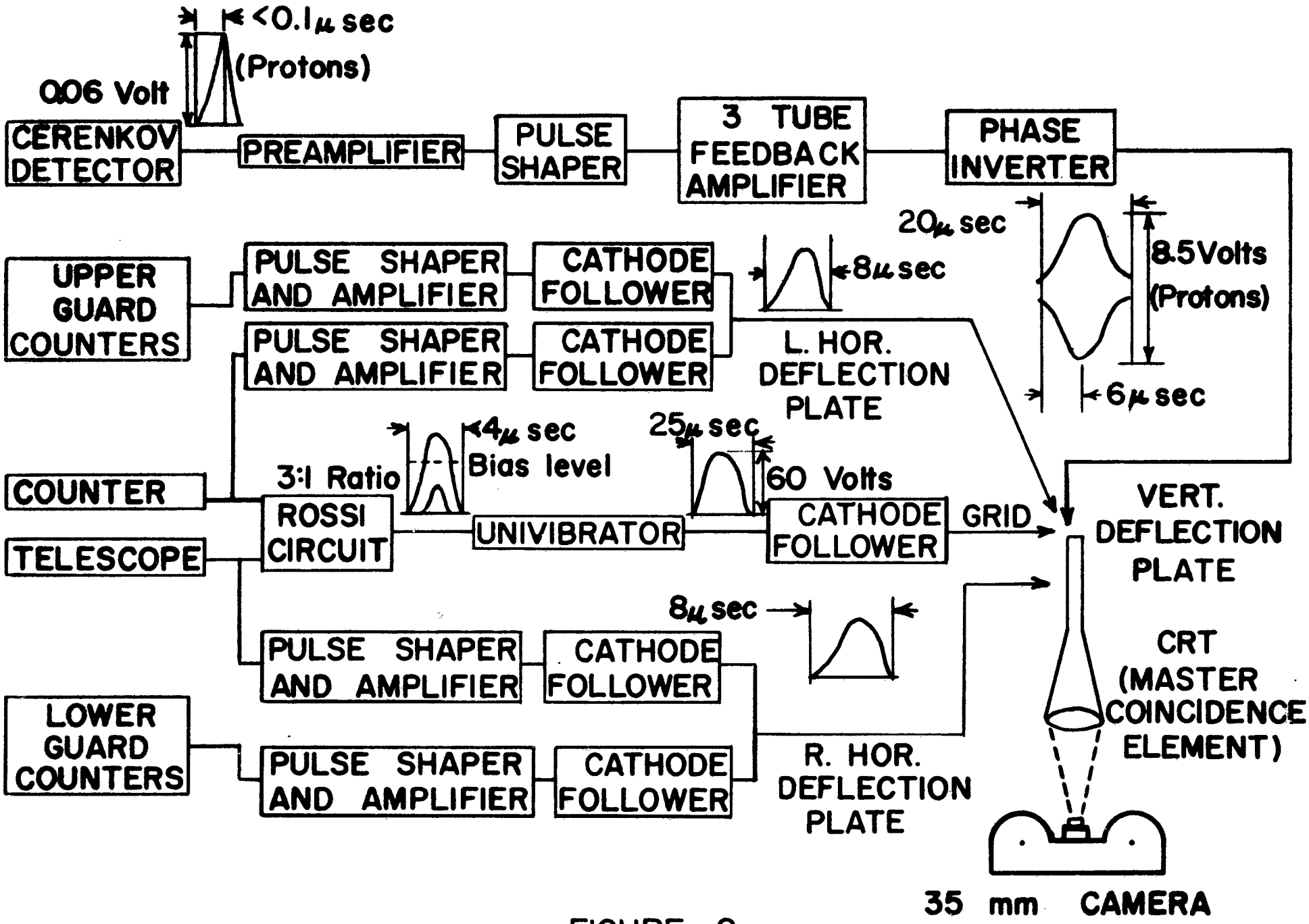
<0.1μ sec
(Protons)
.006 Volt
CERENKOV DETECTOR
PREAMPLIFIER
PULSE SHAPER
3 TUBE FEEDBACK AMPLIFIER
PHASE INVERTER
20μ sec
8.5 Volts
(Protons)
6μ sec
UPPER GUARD COUNTERS
PULSE SHAPER AND AMPLIFIER
CATHODE FOLLOWER
8μ sec
PULSE SHAPER AND AMPLIFIER
CATHODE FOLLOWER
L. HOR. DEFLECTION PLATE
4μ sec
Bias level
25μ sec
60 Volts
COUNTER
3:1 Ratio
ROSSI CIRCUIT
UNIVIBRATOR
CATHODE FOLLOWER
GRID
VERT. DEFLECTION PLATE
TELESCOPE
8μ sec
PULSE SHAPER AND AMPLIFIER
CATHODE FOLLOWER
CRT (MASTER COINCIDENCE ELEMENT)
LOWER GUARD COUNTERS
PULSE SHAPER AND AMPLIFIER
CATHODE FOLLOWER
R. HOR. DEFLECTION PLATE
35 mm CAMERA

FIGURE 2

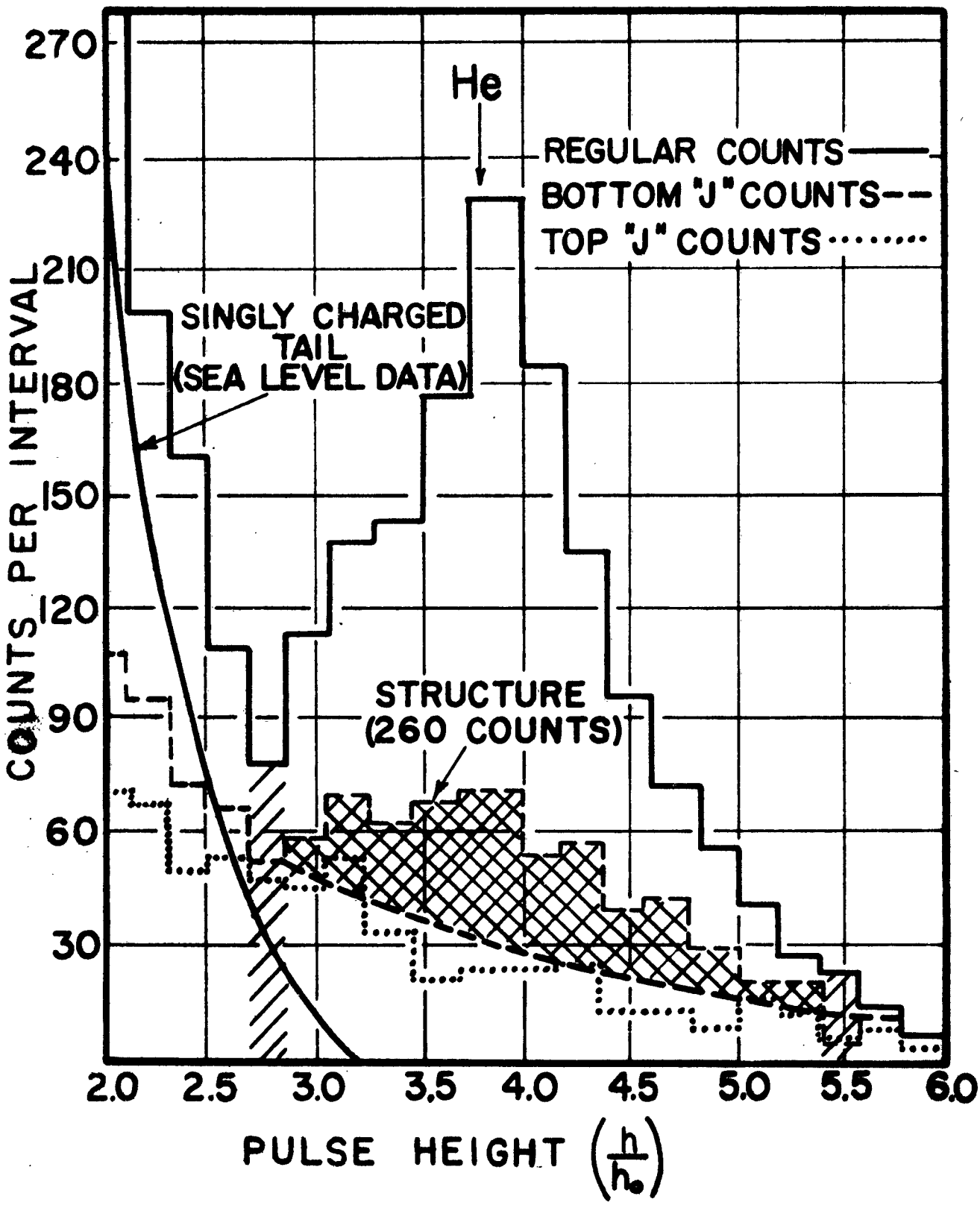
270
240
210
180
150
120
90
60
30
COUNTS PER INTERVAL
He
REGULAR COUNTS
BOTTOM "J" COUNTS
TOP "J" COUNTS
SINGLY CHARGED
TAIL
(SEA LEVEL DATA)
STRUCTURE
(260 COUNTS)
2.0
2.5
3.0
3.5
4.0
4.5
5.0
5.5
6.0
PULSE HEIGHT (h/h₀)

FIGURE 3

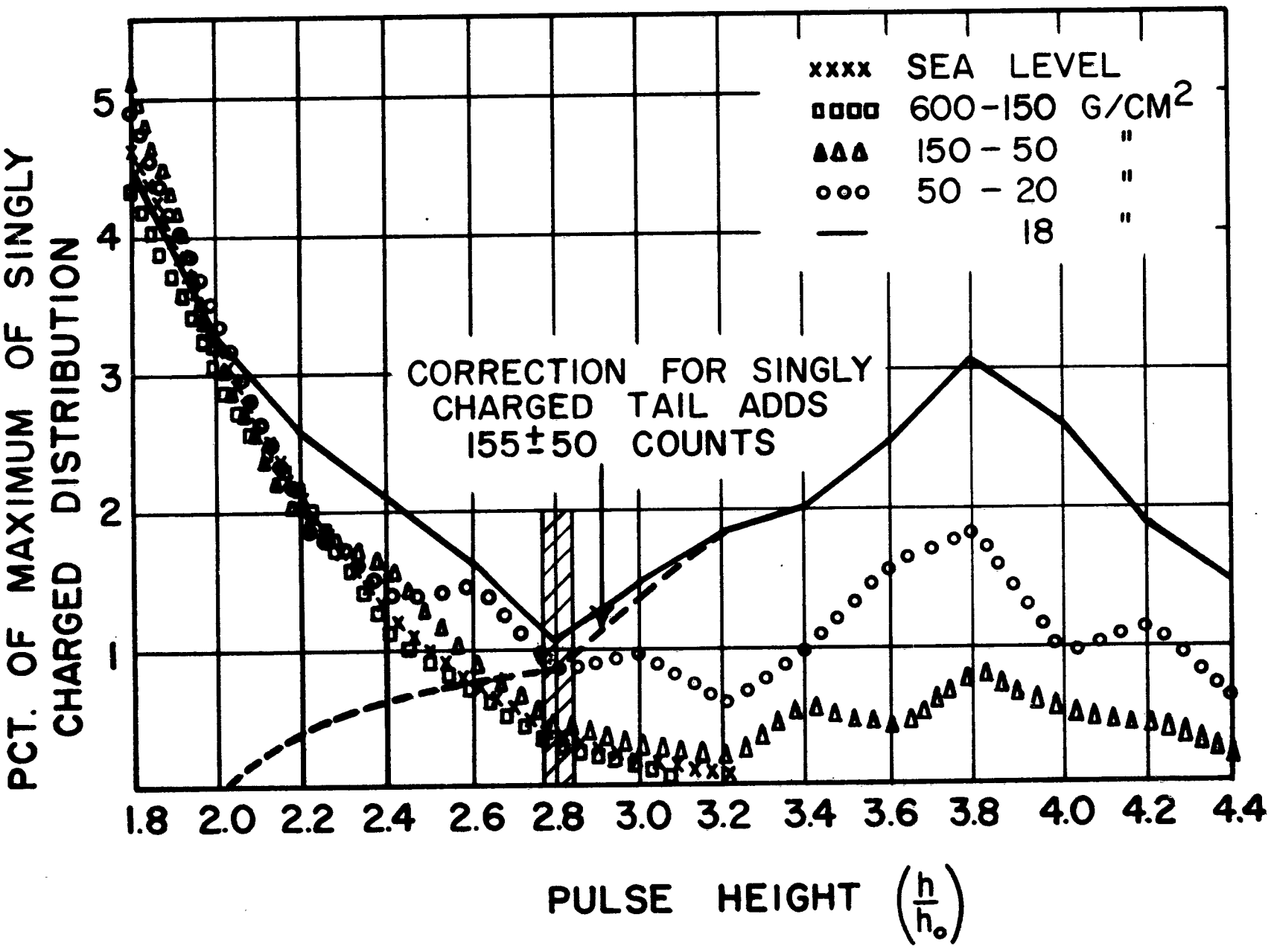
xxxx SEA LEVEL
□□□□ 600-150 G/CM²
ΔΔΔ 150-50 "
ooo 50-20 "
— 18 "
CORRECTION FOR SINGLY CHARGED TAIL ADDS 155±50 COUNTS
PCT. OF MAXIMUM OF SINGLY CHARGED DISTRIBUTION
1
2
3
4
5
1.8 2.0 2.2 2.4 2.6 2.8 3.0 3.2 3.4 3.6 3.8 4.0 4.2 4.4
PULSE HEIGHT (h/h₀)

FIGURE 4

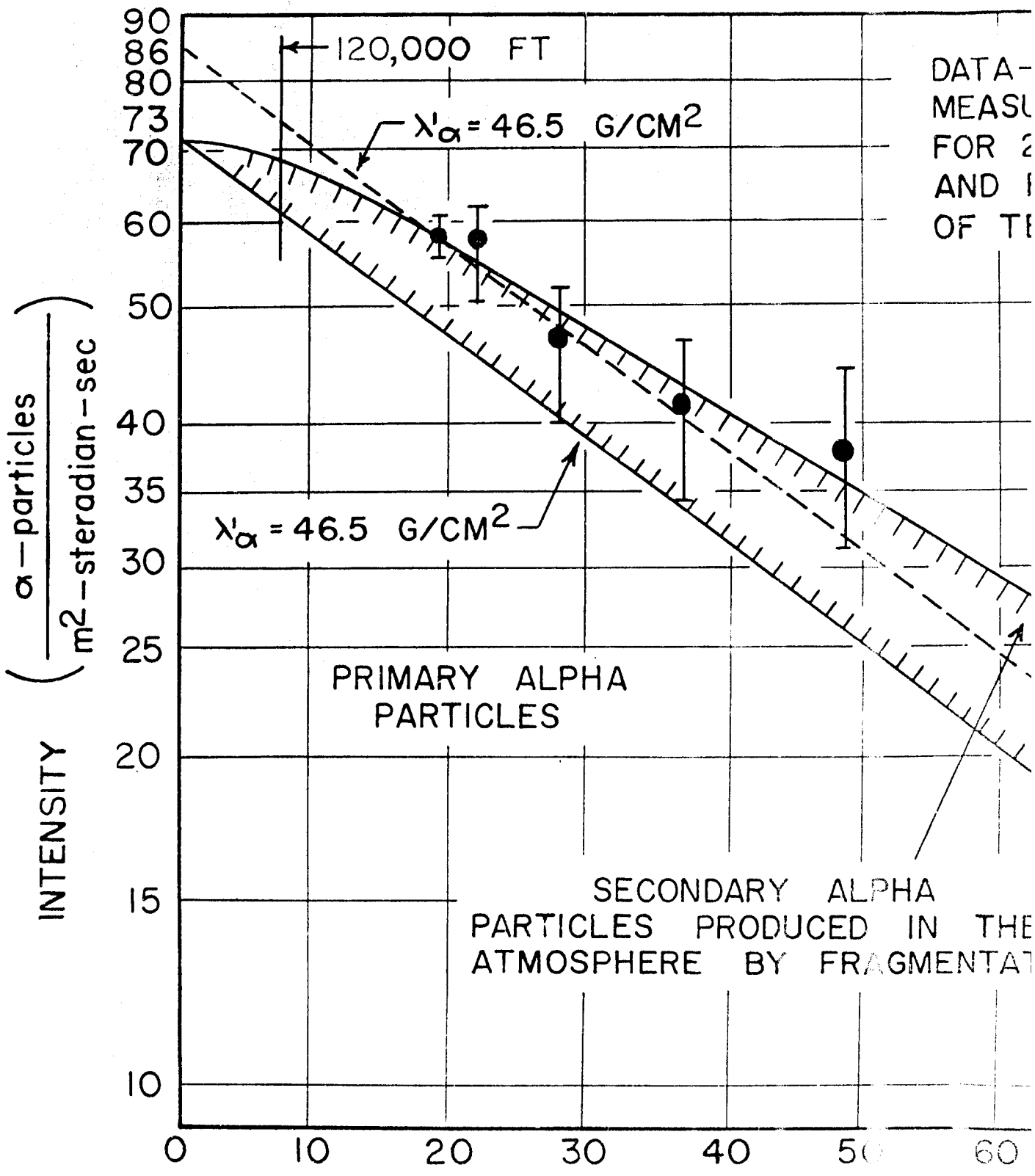

(1)

FIGURE 5

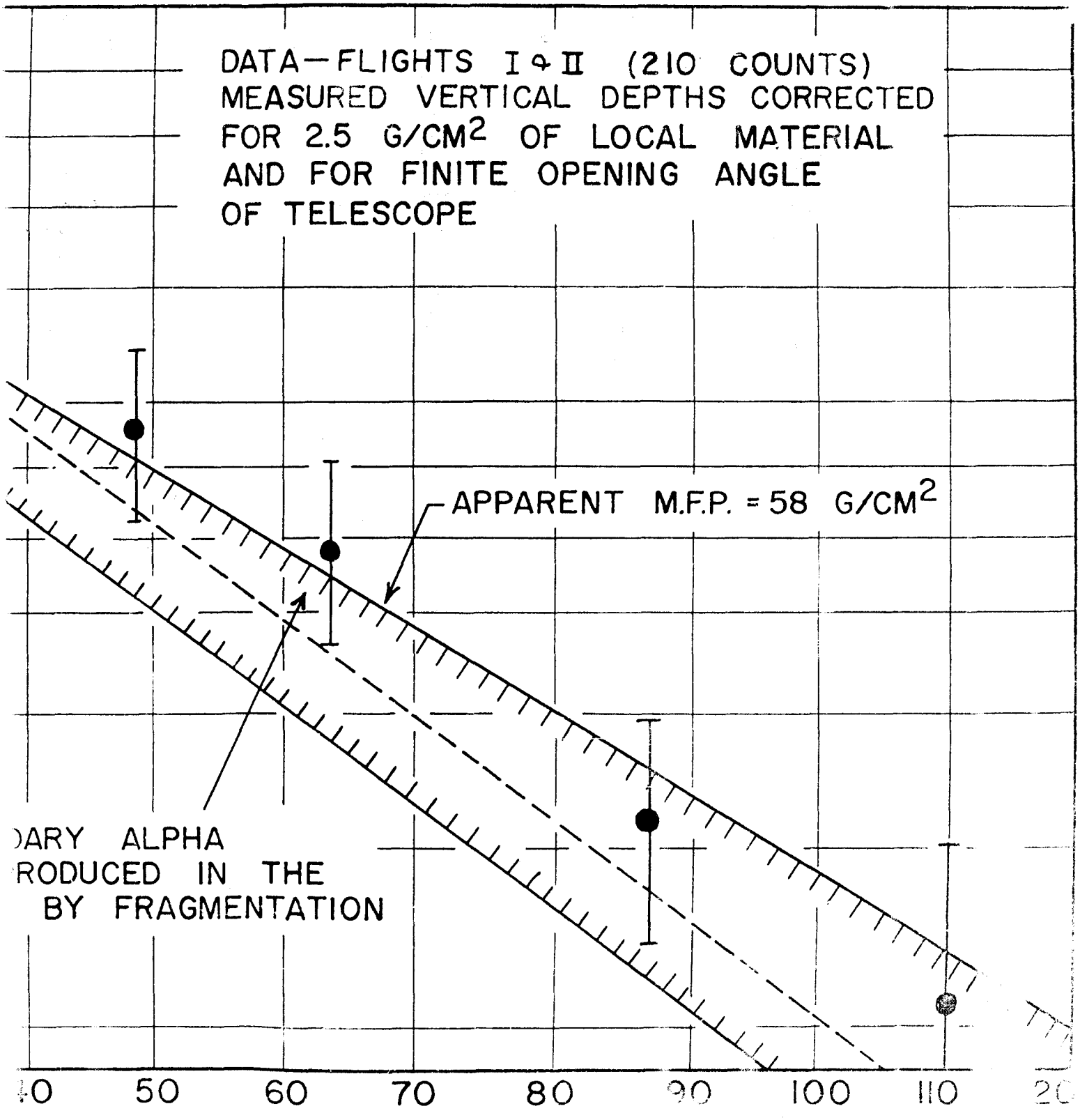
DATA—FLIGHTS I & II (210 COUNTS)
MEASURED VERTICAL DEPTHS CORRECTED
FOR 2.5 G/CM2 OF LOCAL MATERIAL
AND FOR FINITE OPENING ANGLE
OF TELESCOPE
APPARENT M.F.P. = 58 G/CM2
)ARY ALPHA
RODUCED IN THE
BY FRAGMENTATION
40
50
60
70
80
90
100
110
MOSPHERIC DEPTH G/CM2

FIGURE 5

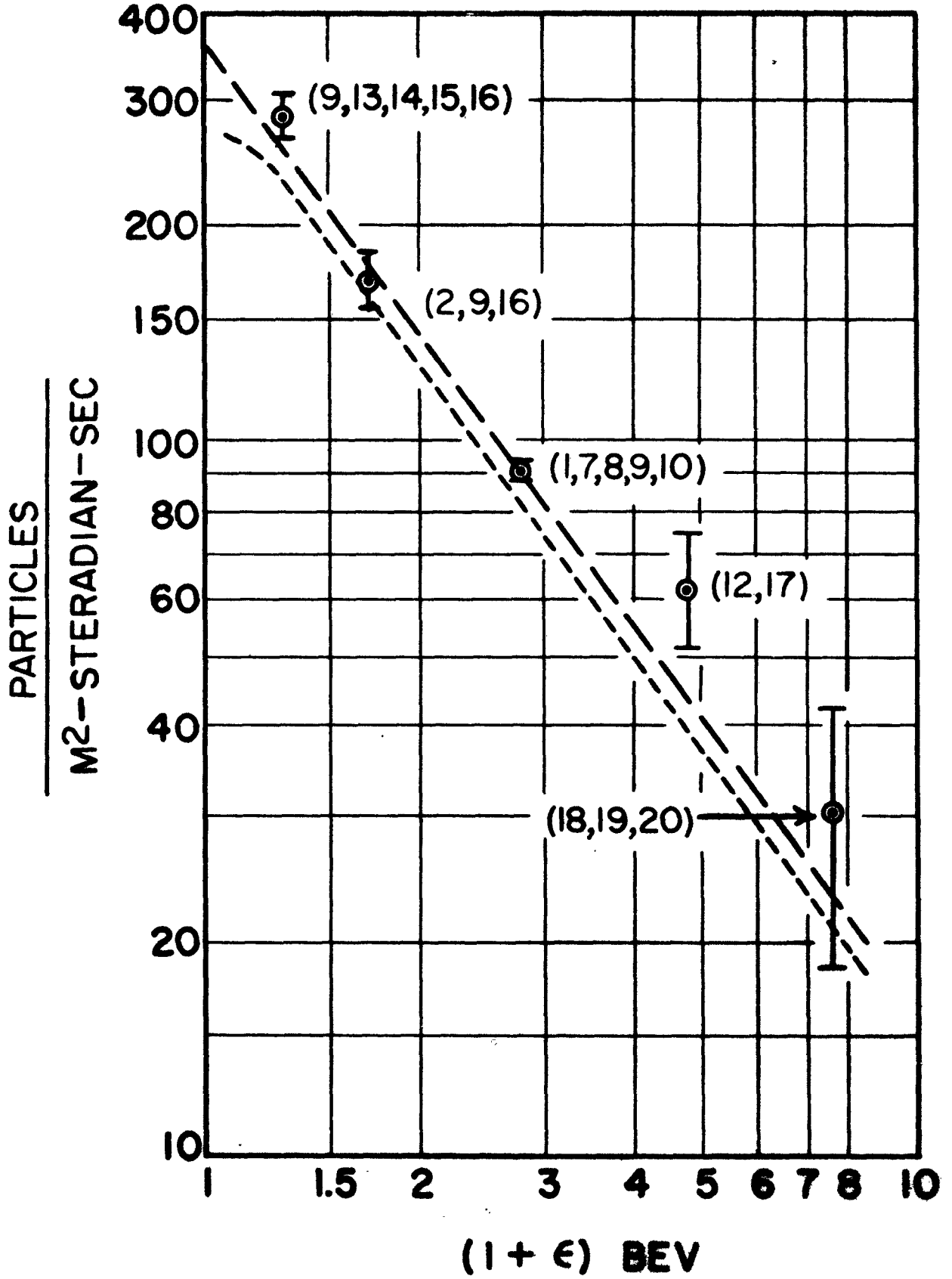
400
300
200
150
100
80
60
40
20
10
(9,13,14,15,16)
(2,9,16)
(1,7,8,9,10)
(12,17)
(18,19,20)
1
1.5
2
3
4
5
6
7
8
10
PARTICLES
M2-STERADIAN-SEC
(1 + ϵ) BEV

FIGURE 6

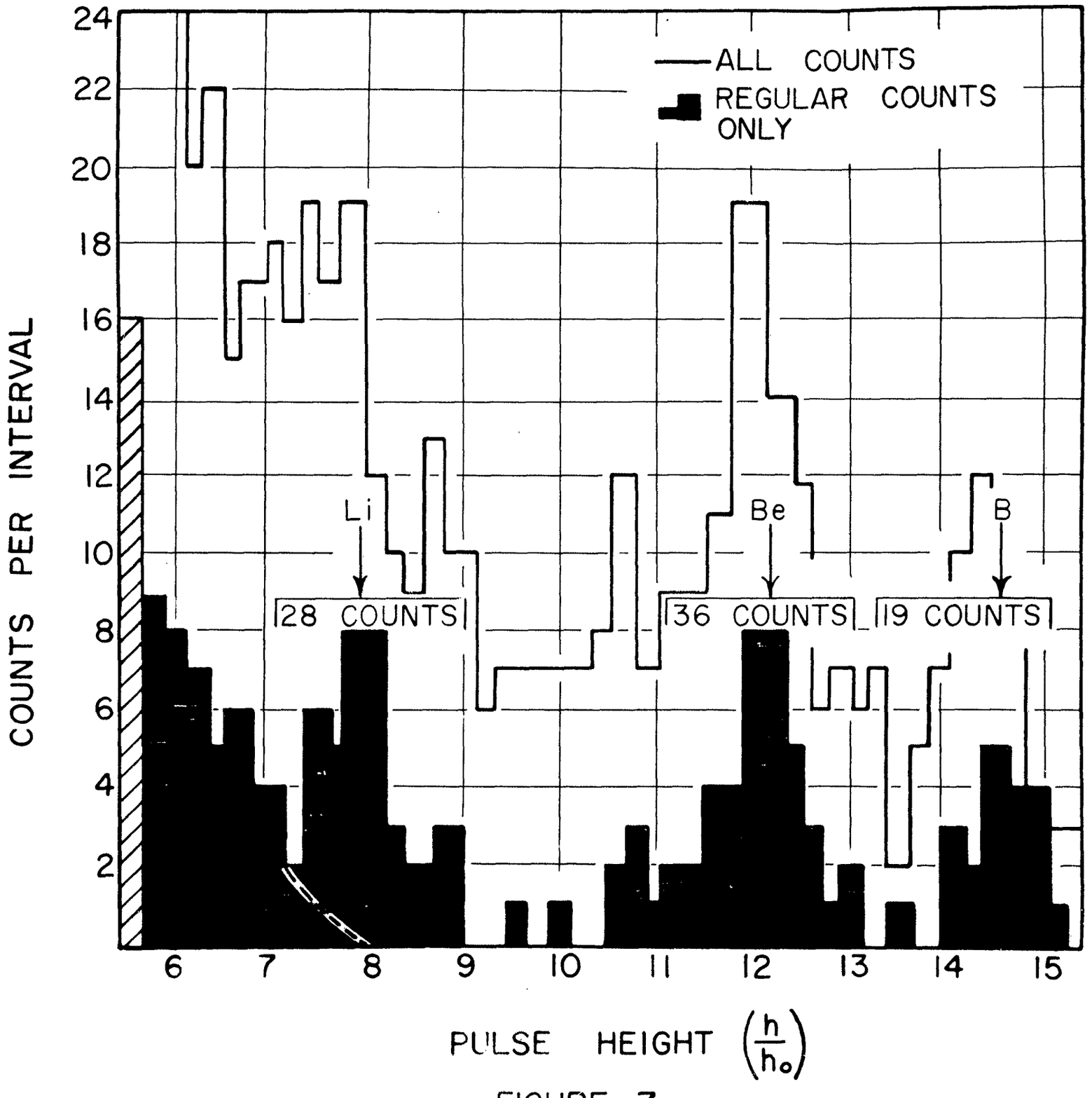
ALL COUNTS
REGULAR COUNTS ONLY
Li
Be
B
28 COUNTS
36 COUNTS
19 COUNTS
COUNTS PER INTERVAL
PULSE HEIGHT (h/h₀)
24
22
20
18
16
14
12
10
8
6
4
2
6
7
8
9
10
11
12
13
14
15

FIGURE 7

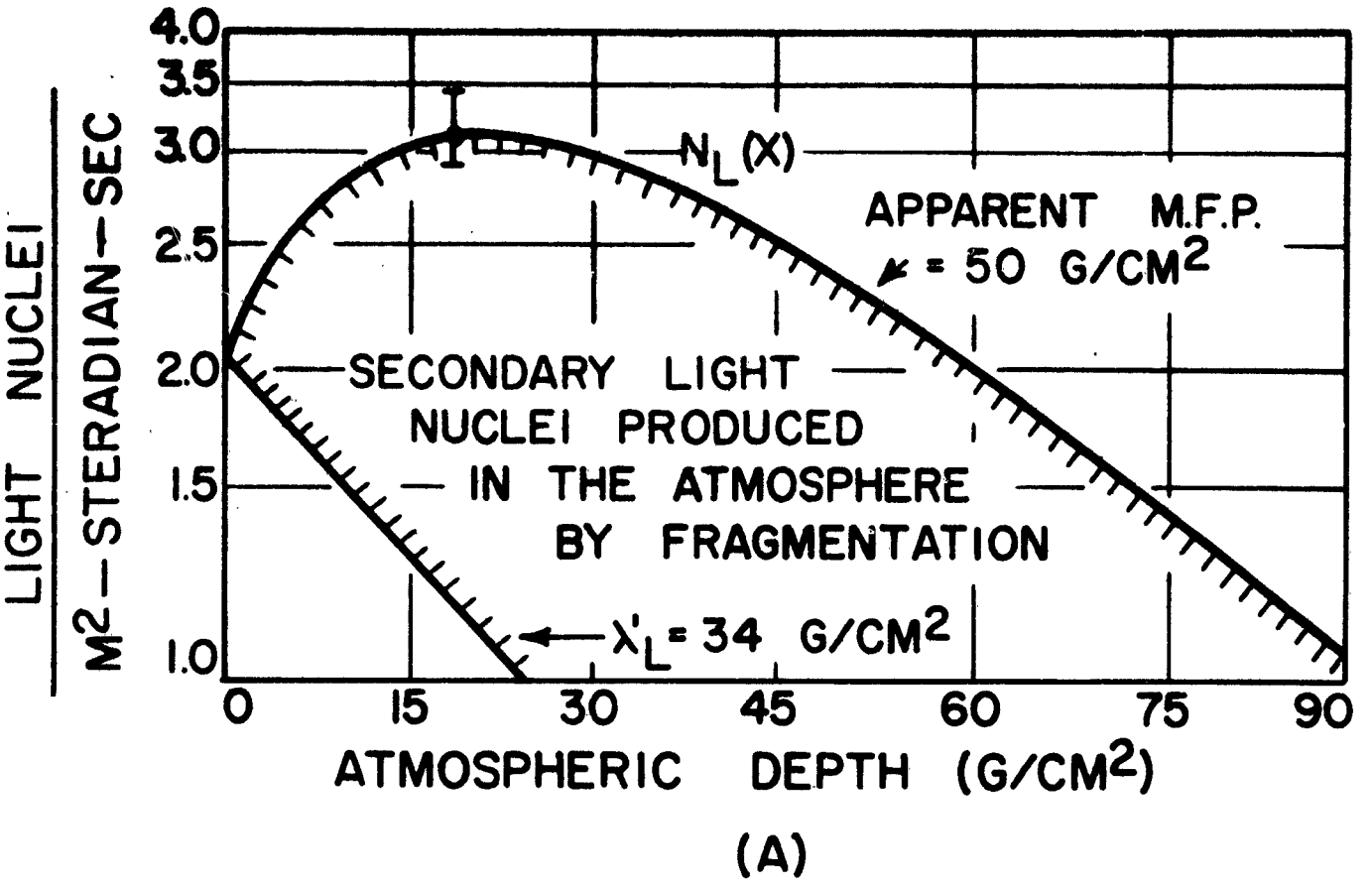
LIGHT NUCLEI
M²—STERADIAN—SEC
4.0
3.5
3.0
2.5
2.0
1.5
1.0
N_L(X)
APPARENT M.F.P.
= 50 G/CM²
SECONDARY LIGHT
NUCLEI PRODUCED
IN THE ATMOSPHERE
BY FRAGMENTATION
λ'_L = 34 G/CM²
0
15
30
45
60
75
90
ATMOSPHERIC DEPTH (G/CM²)

(A)

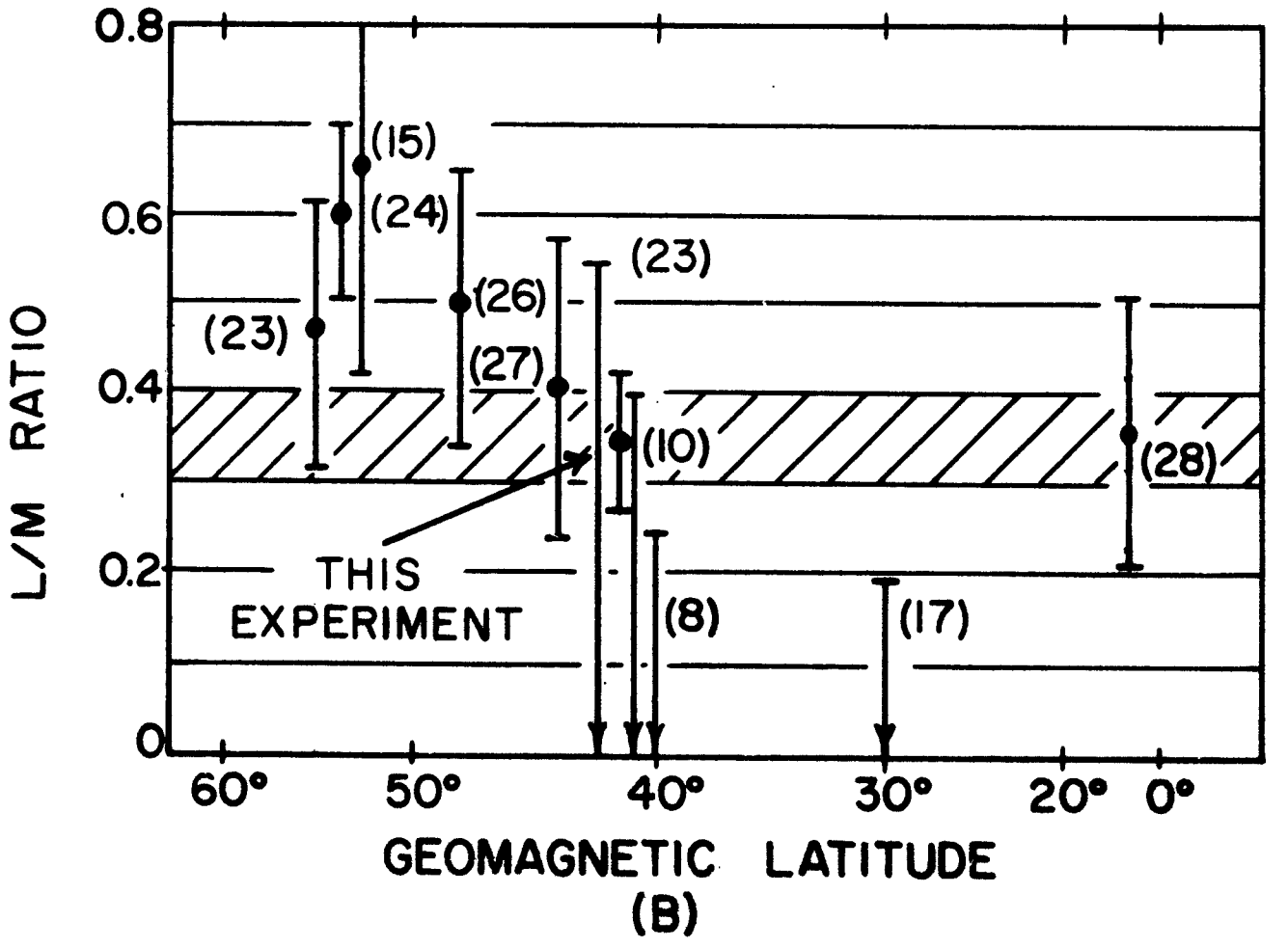
L/M RATIO
0.8
0.6
0.4
0.2
0
(15)
(24)
(23)
(26)
(23)
(27)
(10)
(28)
THIS
EXPERIMENT
(8)
(17)
60°
50°
40°
30°
20°
0°
GEOMAGNETIC LATITUDE

(B)

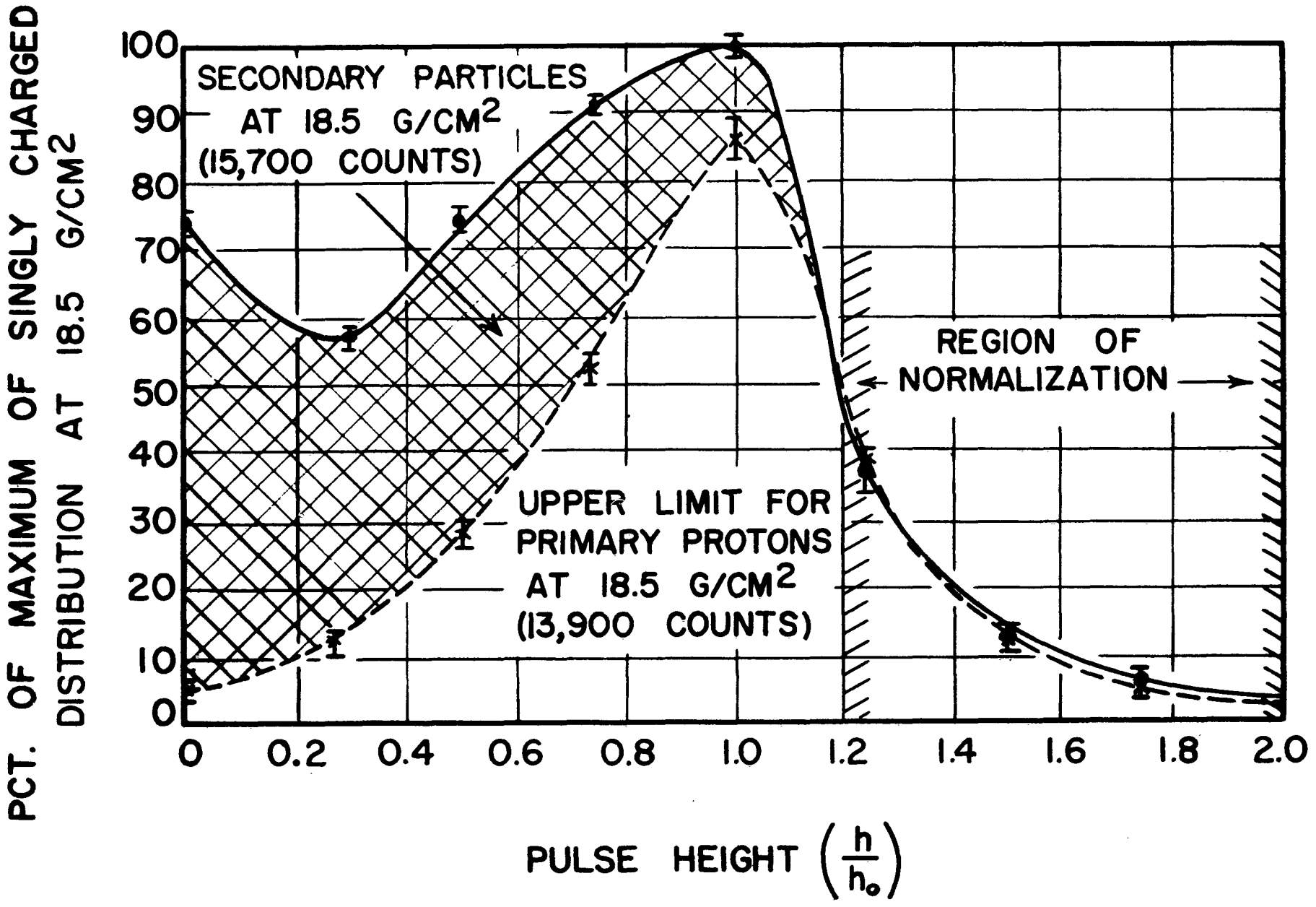
PCT. OF MAXIMUM OF SINGLY CHARGED DISTRIBUTION AT 18.5 G/CM2
100
90
80
70
60
50
40
30
20
10
0
SECONDARY PARTICLES AT 18.5 G/CM2 (15,700 COUNTS)
REGION OF NORMALIZATION
UPPER LIMIT FOR PRIMARY PROTONS AT 18.5 G/CM2 (13,900 COUNTS)
0
0.2
0.4
0.6
0.8
1.0
1.2
1.4
1.6
1.8
2.0
PULSE HEIGHT (h/h0)

FIGURE 9